Review

Detecting single base substitutions, mismatches and bulges in DNA by temperature gradient gel electrophoresis and related methods

Roger M. Wartell[*], Seyed Hosseini, Sandra Powell, Jian Zhu

School of Biology, Georgia Institute of Technology, Atlanta, GA 30332, USA

Abstract

Temperature gradient gel electrophoresis (TGGE) and related methods can separate DNA fragments that differ by a single base pair or defect. This article describes the basic features of TGGE, and reviews the theoretical model of DNA unwinding and its ability to predict DNA mobility in a temperature gradient gel. Recent applications of TGGE and related methods that were directed at detecting point mutations, and evaluating the effects of single site defects are also reported. © 1998 Elsevier Science B.V.

Keywords: Reviews; Temperature gradients; DNA

Contents

[*]Corresponding author.

1. Introduction

Temperature gradient gel electrophoresis (TGGE) and related denaturing gel electrophoretic methods such as denaturing gradient gel electrophoresis (DGGE) can separate DNA fragments which differ at a single base pair site. TGGE exploits two physical properties of DNA; the effect of base pair sequence on the temperature induced unwinding or ''melting'' transition, and the influence of partial denaturation on electrophoretic mobility. In a typical experiment a DNA fragment migrates into a gel with a superimposed temperature gradient until it reaches a temperature which induces partial strand unwinding. As a consequence of being partially denatured, the DNA undergoes a large decrease in gel mobility. Homologous DNAs with a single base pair difference in their least stable region migrate to different depths before undergoing abrupt changes in mobility. DGGE simulates the temperature gradient by employing gels with a gradient of the chemical denaturants urea and formamide.

In this paper we review the basic features of TGGE, and recent results obtained by TGGE, DGGE, and variations of these two methods. We examine the theoretical model of DNA denaturation, and how it is used with TGGE to detect and/or characterize single base pair substitutions, mismatches, and bulges in DNA fragments. Previous reports have reviewed earlier work on the methodology and applications of TGGE [1] and DGGE [2–5]. Denaturing gel methods have been primarily employed as tools to screen for mutations or polymorphisms in DNA fragments amplified by the polymerase chain reaction [6], or genomic restriction fragments that are hybridized to labeled probes [7]. They have also been applied in thermodynamic studies on the influence of specific mismatches, bulges, and base pair substitutions on the stability of long DNA [8,9]. Results from both types of applications are described.

An advantage of TGGE is that a theoretical understanding governing the electrophoretic separation of two DNAs differing by a base pair substitution or defect is reasonably well understood. DNA melting theory [10,11] and an empirical model of how partial denaturation effects DNA gel mobility [2] have been used to develop computer simulations

for selecting DNA fragments for TGGE, planning experiments, and interpreting results [3,12,13]. A few studies have indicated occasional discrepancies between the predicted separation of two DNA fragments in a denaturing gel and experimental observations [14–16]. Since computer simulations are often used to guide experiments, an understanding of the underlying theory and its limitations is an important consideration. We review the assumptions made in applying DNA melting theory to denaturing gel conditions, and possible causes for unexpected behavior.

2. Background

2.1. Experimental features of temperature gradient gel electrophoresis

Denaturing gel electrophoresis experiments are carried out using polyacrylamide slab-gels. DGGE employs gels with a gradient of chemical denaturant, and electrophoresis occurs in a bath maintained at 60°C. TGGE uses a gel with a uniform concentration of chemical denaturant, and has a superimposed temperature gradient. Both approaches give similar, but not necessarily identical results. Several articles have provided detailed descriptions of denaturing gradient gel electrophoresis [4,5]. Here we emphasize temperature gradient gel electrophoresis. TGGE provides a more direct comparison with theoretical predictions of temperature induced DNA melting and its influence on gel mobility.

Temperature gradient gel electrophoresis experiments have employed both vertical and horizontal slab-gel systems. The first temperature gradient gel system described in the literature was a vertical apparatus that was applied to studies of protein and nucleic acid denaturation [17]. A horizontal TGGE apparatus was introduced and applied by Rosenbaum and Riesner [18]. The polyacrylamide gel in this system is cast on a thin supporting sheet that is placed on a horizontal metal plate that establishes the temperature gradient. We have employed a vertical TGGE system that was developed from a conventional vertical gel apparatus [19]. The apparatus was modified to allow the glass plates containing the polyacrylamide gel to be sandwiched between two

metal blocks. Channels drilled through the blocks are connected to two thermostated fluid circulators set at different temperatures. Fluid flow establishes a temperature gradient from top to bottom or from one side to the other depending on the orientation of the channels to the direction of electrophoretic migration (Fig. 1). The surface dimensions of the gel are about 19 cm by 20 cm.

The polyacrylamide gels in our studies utilized a mixture of acrylamide–bisacrylamide (37.5:1, v/v) at concentrations of 6.5 to 8%. The solvent of the acrylamide solution and the running buffer was 0.5× TBE; 0.045 *M* Tris–borate, pH=8.0, 1 or 2 m*M* sodium EDTA. The gel solutions were prepared by mixing appropriate volumes of a 30% aqueous solution of acrylamide–bisacrylamide, solid urea, deionized formamide and concentrated TBE. The

urea and formamide lower the thermal stability of duplex DNA to a convenient temperature range. We commonly employed gels containing 58% denaturant, where 100% denaturant equals 7 *M* urea and 40% (v/v) formamide. Under this condition, DNA segments varying in GC content from 40 to 60% unwind at temperatures between 28 and 55°C. Tris–acetate [1] and 3-(*N*-morpholino)propanesulfonic acid (MOPS) [16] buffers have also been employed in TGGE experiments. DNA bands are observed after an electrophoretic run by ethidium bromide or silver staining or by employing radioactively labeled probes.

2.1.1. Perpendicular and parallel formats

TGGE (or DGGE) experiments can be carried out with the migration of DNA bands perpendicular or
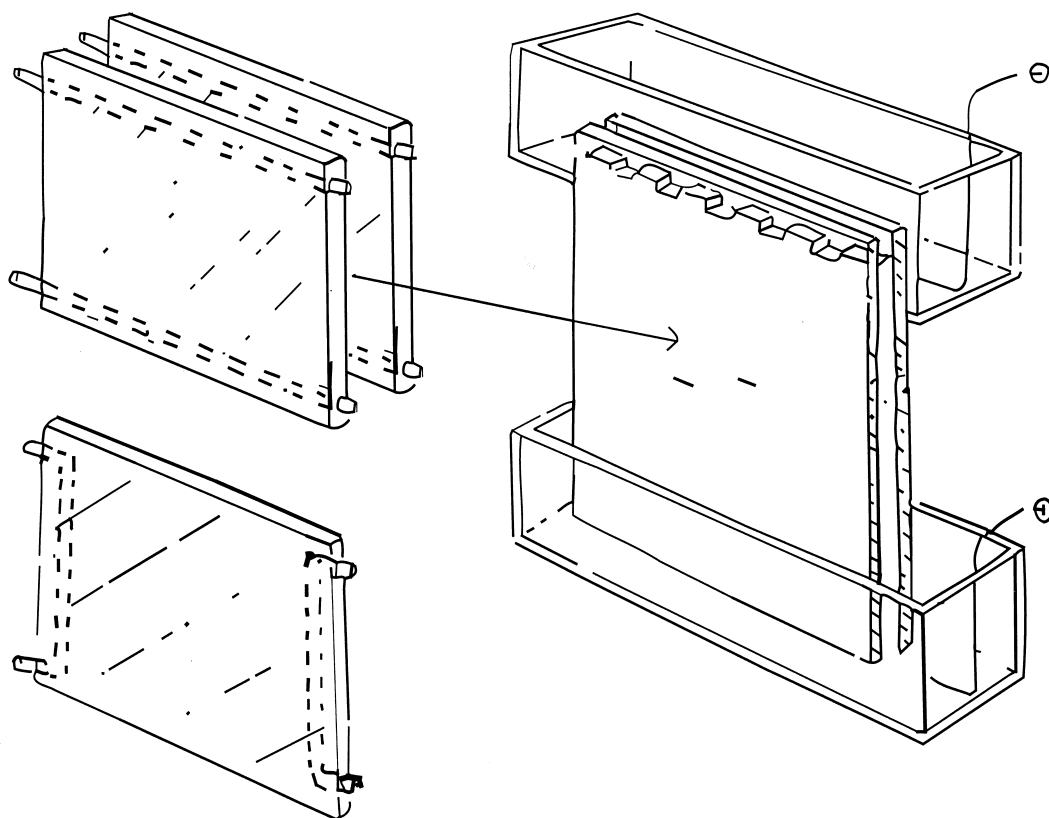
Fig. 1. A sketch of a vertical TGGE apparatus. Modifications of the conventional vertical gel apparatus enable the glass plates containing the acrylamide gel to be sandwiched between two aluminum heating blocks [19]. Channels (shown by dash lines) in the heating blocks allow circulating fluid to establish a temperature gradient from the top to the bottom (parallel to the running direction) or from one side to the other (perpendicular to the direction of electrophoresis). Two thermostated fluid circulators are employed to set the high and low temperatures.

parallel to the temperature (or chemical) gradient. Fig. 2a,b illustrates results using the two formats. The parallel TGGE format shown in Fig. 2a is generally used to screen for base pair (bp) changes in multiple DNA samples. The two bands in each lane are from EcoRI/Rsa I double digests of homologous pUC8-modified plasmids [19]. The upper bands correspond to 676 bp fragments identical in sequence. The lower bands correspond to homologous 373 bp DNAs differing by single base pair substitutions. Lane 5 contains the 373 bp DNA with the wild type sequence, while the other lanes have DNAs with single GC to AT substitutions. The base pair differences are all located within the 50 bp end-segment that forms the least stable portion of the 373 bp sequence. The GC to AT substitutions decrease the overall stability of this segment, and lower the temperature required for its denaturation.

The differing depths to which the DNAs with GC to AT substitutions migrate demonstrate the influence of nearest neighbor stacking interactions on DNA stability. TGGE mobility differences have also been observed for DNAs with either AT to TA or GC to CG base pair substitutions [8]. The distance separating two DNAs differing by a single base pair substitution varies with the details of the experiment, but distances of 2 to 15 mm are commonly observed. Single defects such as mismatches and bulges decrease the stability of a DNA more than a GC to AT change and result in larger separations [2,8,9]. Heteroduplex DNAs formed by melting and annealing wild type DNA with a test DNA fragment provide the most sensitive means of detecting mutations or polymorphisms [1,4]. The influence of single site mismatches and bulges on DNA stability is described more fully in Section 3.3.

While the parallel TGGE format provides a straightforward approach for screening multiple samples, the perpendicular TGGE format provides a better approach for analyzing the unwinding behavior of a given DNA. The multistep mobility curve of the 373 bp DNA shown in Fig. 2b illustrates several common features of a perpendicular TGGE experiment. In region I the DNA migrates as an intact double helix. Its mobility depends on its length, and any sequence induced curvature of its helix axis [20]. The quasilinear increase in mobility of the DNA may be attributed to the effect of
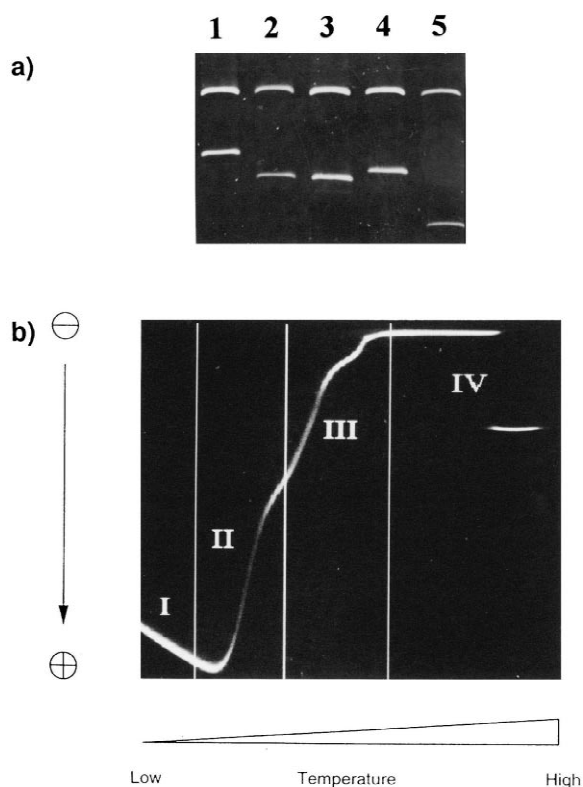

Fig. 2. (a) Parallel TGGE experiment. The temperature gradient is 4°C parallel to the direction of electrophoresis, 29 to 33°C. The experiment was run at a constant voltage of 80 V for 14.5 h. The samples were DNA plasmids treated with Rsa I/EcoR I enzymes. For each lane, the top band is the 676 bp DNA and the bottom one is the 373 bp DNA. Lanes and plasmids: (1) pUC8−5, (2) pUC8−36, (3) pUC8+3, (4) pUC8−15, (5) pUC8−31, the wild type. The plasmids in lanes 1 to 4 differed with pUC8−31 by single base pair change (G→A) in the first melting domain of the 373bp DNA. The locations of mutations for pUC8−5, pUC8−36, pUC8+3 and pUC8−15 are 48, 17, 55 and 38 base pairs away from the duplex end with the EcoR I site, respectively [19]. (b) Mobility curve of the wild type 373 bp DNA using perpendicular TGGE. The temperature gradient is from 15 to 60°C across the gel perpendicular to the direction of electrophoresis. The run was for 12 h at 120 V. Four distinct melting regions are shown. In region I the DNA is not yet melted, and its mobility increases slightly with temperature. Region II contains the first transition step which is correlated with the first melting step in the melting map. Region III shows two further melting steps. Region IV includes the later stages of the transition. Both partial duplex and the faster moving band assigned to single stranded DNA can be observed in a 1.5°C wide temperature zone.

increasing temperature on gel viscosity and/or gel pore size. The phenomena is observed in both vertical [8,19] and horizontal [1] temperature gradient systems, but is not observed in chemical gradient gels [2].

The decrease in mobility observed in region II of Fig. 2b is attributed to a transition from completely duplex molecules to molecules in which the least stable segment is denatured. The single stranded portions of the partially melted molecules can form branches which hinder movement through the gel pores. The second and third mobility steps observed in region III of Fig. 2b are attributed to the unwinding of more stable segments and the concomitant increase in the portion of single strands. Interpretation of these regions of the mobility curve is based on theoretical and experimental studies of equilibrium DNA melting in solution (see below). Studies show that DNA molecules longer than 100 bp tend to unwind in a succession of segments or blocks of base pairs as the temperature is slowly raised [10,11]. The segments are often referred to as "melting domains". Each domain unwinds as a cooperative unit over a narrow temperature interval (~2°C), and contains from thirty to several hundred contiguous base pairs. This view of DNA unwinding, the successive opening of domains, provides a useful but incomplete picture of a DNA melting transition. All partially melted DNA microstates and duplex-to-strands dissociation are considered in the statistical mechanical model which describes DNA melting [2,10,11].

The single continuous DNA band observed in regions II and III of Fig. 2b implies that the rates for denaturation/renaturation of the melting domains are fast relative to differences in migration velocities of the partial duplex conformations. The relative mobility of the DNA at a given temperature can be related to its average conformation. We note that under very low electric field strengths, DGGE experiments have shown two distinct bands within a denaturant range that induces melting of an interior domain [21]. The more retarded band corresponds to that expected with the interior domain fully unpaired. The less retarded band appears to be due to metastable conformations that are observed under these conditions.

Region IV of Fig. 2b reflects the further unwinding of the partial duplex molecules and the dissociation from partial duplex to two single strands. Two bands are observed within a ~1.5°C temperature range, the more retarded band decreasing in concentration, and the faster moving band increasing in concentration. The faster moving band is attributed to the denatured single strands. The presence of the two bands indicates that in this temperature zone both partial duplex and single strands coexist and the rates of duplex-to-strands dissociation/reassociation are slow relative to the difference in migration velocities of the single strands and partial duplex.

In order to detect a single base pair change between two DNA fragments, the base pair should be located in a melting domain that unwinds at a temperature below the onset of duplex-to-strands dissociation [4,22,23]. For the 373 bp DNA, the mobility curve of Fig. 2b indicates three melting domains in regions II and III; the first and second domains are separated from the long mobility plateau by a smaller step in mobility change. The first two melting domains appear to be well separated from the strand dissociation step. This stepwise melting of early melting domains is not always observed for DNA fragments. For mobility curves with one sigmoidal transition, the separation between the first melting domain and the onset of strands dissociation is not apparent. Visual inspection of region IV suggests that the strands dissociation reaction occurs only over the double band temperature zone. This interpretation may be misleading. The onset of strands dissociation may be occurring at a lower temperature. Whether one actually observes separation of single strands from partial duplex depends on the rates of the duplex-strands reaction, the molecules' migration velocities, as well as the sensitivity of staining single strands. The association/dissociation rates for the duplex-strands reaction may be influenced by the solvent, temperature, and the sequence of the strands.

2.2. Theoretical analysis of DNA denaturation and gel mobility

2.2.1. Basic model

Theoretical algorithms have been developed to calculate the melting behavior of DNA molecules of known sequence [10,11,13]. When combined with a

model of how DNA melting affects electrophoretic mobility, melting calculations can predict the mobility of a DNA molecule relative to a complete duplex as a function of temperature. Lerman et al. [2] proposed that the electrophoretic mobility of a partially melted DNA decreases exponentially with an increase of its melted region. At temperature T the mobility of a DNA fragment, $\mu(T)$, relative to the mobility of the completely helical DNA, $\mu_o(T)$, is given by $\mu(T)=\mu_o(T) \exp[-p(T)/L]$. $p(T)$ is the calculated number of open base pairs at temperature T, and L is the length of a flexible unit of DNA strand. This equation is not expected to accurately predict mobility curves beyond the initial stages of melting. Although a systematic study has yet to be reported, the equation has produced good agreement with mobility curves of a few DNAs in perpendicular TGGE [9] and DGGE [24] experiments.

The model employed in the analysis of DNA unwinding assumes that each base pair is in one of two states; stacked with Watson–Crick hydrogen bonds, or disordered. The intrinsic stability of each base pair is assumed to depend on its base pair type and the stacking interactions with neighboring base pairs [10]. A slightly different model [11] has been adopted by Lerman and collaborators in which only nearest neighbor stacking interactions govern base pair stability. Both formulations produce the same results for DNAs longer than ~50 bp. The model also includes the entropy difference between unwinding an end domain vs. melting an internal domain of the same size and sequence, and the duplex-strands dissociation reaction. The average properties of a given sequence at a specific temperature are calculated from the equilibrium statistical mechanical analysis of all allowable states.

2.2.2. Melting maps and melting curves

Melting maps are frequently calculated to predict the stability distribution of a sequence and the location of the low melting regions where mutations and other sequence alterations may be detected [3]. A melting map displays the midpoint temperature, T_m, for each individual base pair in a DNA fragment. The T_m of a base pair, the temperature at which the base pair's probability of being disordered or open, is 0.5. Fig. 3 shows calculated melting maps for two DNA fragments; the 373 bp DNA fragment em-
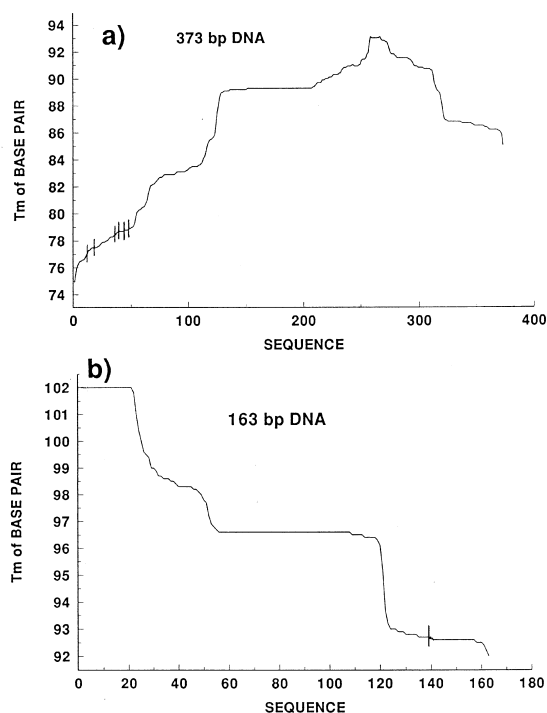

Fig. 3. Melting maps of two DNA fragments. (a) The 373 bp DNA fragment employed in the experiments shown in Fig. 2, and (b) the 163 bp DNA fragment containing part of the rpsL gene of *Mycobacterium smegmatis*. The vertical tick marks intersecting the melting map curves indicate the locations of base pair changes that have been detected. The single tick mark in the 163 bp DNA curve corresponds to four base pair changes within a codon.

ployed in the experiment shown in Fig. 2, and a 163 bp DNA fragment containing part of the rpsL gene of the *Mycobacterium smegmatis* bacteria. Mutations in the rpsL gene confer resistance to the antibiotic streptomycin. Some results with this fragment are described below.

T_m values in Fig. 3 were evaluated by calculating the probability of being disordered for each base pair at 0.1°C intervals throughout the melting region. Calculations were made assuming a solvent of 0.1 M Na$^+$. The tendency of DNA to unwind by a succession of domains is displayed by the melting maps. Fig. 3a shows that the least stable domain of the 373 bp DNA is the segment approximately fifty base pairs from the EcoRI or left end of the sequence. The second melting domain is adjacent to the first. It extends from sequence position 50 to about 115 with an average T_m of about 83°C. Two additional

melting domains precede the most stable region located between positions 200 to 300.

Fig. 3b shows that the least stable region of the 163 bp DNA extends about 40 base pairs in from the right end. The 163 bp DNA sequence includes a stretch of 25 GC base pairs or a "GC-clamp" on the left end. GC clamps are placed on one end of a DNA to help produce a low melting domain in the remainder of the molecule (see below). Two melting domains (28–54 and 55–120) are indicated prior to the GC clamp segment on the left end of the molecule. Although highly useful, melting map calculations do not include the duplex-to-strands dissociation reaction, and thus provide an incomplete description of DNA melting behavior. The latter reaction should be considered for DNAs less than 600 bp long to ensure that a melting domain will actually exist.

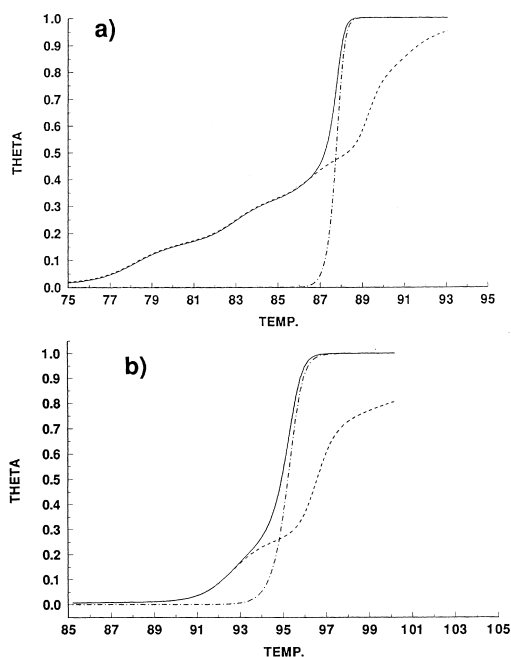Fig. 4 shows calculated melting curves, θ_{tot} vs. temperature, for the 373 bp and 163 bp DNA sequences described in Fig. 3. θ_{tot}, the total fraction of open base pairs, is determined from the product of the fraction of melted base pairs among duplex molecules, θ_d, and the fraction of total strands that have completely dissociated into single strands, θ_{ss} [10]. Plots of θ_d and θ_{ss} are also shown in Fig. 4. θ_d is related to the melting map calculation. It is the sum of the probabilities of melting each base pair for duplex molecules. The melting map and θ_d describe a situation where the most stable portion of the DNA is crosslinked and the strands are unable to dissociate. θ_{ss} corresponds to the "all-or-none" dissociation reaction of duplex molecules to single strands.

The melting curves in Fig. 4 illustrate the importance of considering duplex-strands dissociation on the ability to observe melting domains and detect sequence alterations. The first two melting domains of the 373 bp DNA open prior to any significant contribution of strands dissociation. The predicted third and fourth melting domains do not have an experimental existence since strands dissociation dominates the last part of the melting curve. For the 163 bp DNA, only the first melting domain opens prior to the onset of strand separation.

2.2.3. Assumptions made in applying theory

The parameters used in the calculations for Figs. 3 and 4 were empirically determined from studies of DNA melting in solutions containing 0.075 to 0.1 M Na$^+$ [10,25]. In this range of monovalent cations, good agreement is observed between theoretical predictions and experimental melting curves [10,25,26]. This type of solvent differs from the Tris–borate or Tris–acetate buffers used in a temperature gradient gel. A more appropriate parameter set is difficult to evaluate due to the nonequilibrium nature of DNA transitions in low monovalent cation solvents. When DNA melts in a buffer containing ≤0.02 M Na$^+$, the slow approach to equilibrium for melting certain types of domains, and for the duplex-to-strands dissociation reaction create discrepancies between theoretical predictions and experimental melting transitions [26–28].

Applying melting predictions using the 0.1 M Na$^+$ parameters to TGGE solvent conditions presumes that the relative stability distribution of a DNA sequence does not change with solvent. Although this is not strictly true, experimental results indicate

Fig. 4. Calculated melting curves, θ_{tot} (———), θ_d (- - -), θ_{ss} (– · –) vs. temperature for: (a) the 373 bp DNA, (b) the 163 bp DNA. θ_{tot} is the total fraction of open base pairs, θ_d is the fraction of melted base pairs among duplex molecules and θ_{ss} is the fraction of total strands that have completely dissociated into single strands. $\theta_{tot} = \theta_d \times \theta_{ss}$.

that the main features of a sequence's stability distribution are preserved. DNA melting studies show that the number and relative size of subtransitions in a melting curve do not change drastically between 0.1 and 0.01 M Na$^+$ for fragments shorter than 800 bp [29]. Stacking interactions empirically evaluated in 0.02 M Na$^+$ predict DNA melting transitions similar to those predicted by stacking interactions evaluated in 0.075–0.1 M Na$^+$ solutions [19,23]. A recent study indicates that formamide does not affect the inherent cooperativity of melting domains, and its effect on DNA stability has a small GC dependence [30]. The concentrations of urea employed in TGGE gels also lowers the stability of DNA with little dependence on GC content [31].

The part of a melting transition which appears to change the most between a 0.1 M Na$^+$ solvent and the lower Na$^+$ concentration used in TGGE is the duplex-strands reaction. Kinetic studies and melting curve studies show that below 0.1 M Na$^+$, strands reassociation becomes an increasingly slow process [32,33], leading to highly irreversible melting transitions. This nonequilibrium aspect of DNA melting can be expected to reduce the accuracy of the equilibrium theory's predictions particularly for the duplex-strands reaction. Another factor which can contribute to the nonequilibrium character of the duplex-strands reaction is the ability of the dissociated strands to migrate away from the region of the partial duplex. The reaction volume is not a closed system and the concentration of single strands can decrease. The extent to which this factor influences DNA melting will depend on the voltage and the effects of the gel matrix.

The above considerations suggest that if a DNA fragment is predicted to have the onset of strands dissociation close in temperature to the first melting domain, it may not be applicable for mutation detection. Discrepancies between theoretical expectations and gel experiments may result from an inaccurate assessment of the onset of strand dissociation. If a DNA fragment is predicted to have one or more melting domains well separated from the strands dissociation step, it should be useful for detecting base pair changes.

2.2.4. Predicting DNA fragments for detecting mutations

Predicting a DNA fragment for detecting defects

and mutations involves calculating the melting properties of trial fragments surrounding the region of interest. The objective is to find a fragment in which the region of interest is in the lowest melting domain, and this domain is separated from the onset of strand dissociation. We have employed two criteria to determine when these conditions are met. The first criteria employs melting maps to determine whether the region of interest is in the lowest melting domain. The second criteria requires that the derivative of the calculated melting curve, $d\theta_{tot}/dT$, has at least two peaks separable by at least 1°C. The latter criteria attempts to ensure, within the accuracy of the theory, that the first melting domain is separable from the strands dissociation phase of the transition. Fig. 5 shows examples of derivative melting curves (DMC) for two DNA sequences.

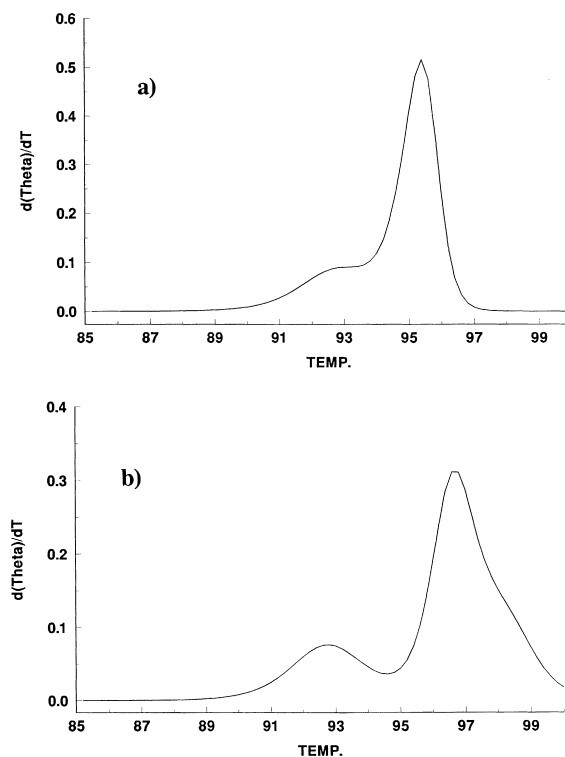A program called MELTSCAN was developed to

Fig. 5. Derivative melting curves are shown for two DNAs containing a 138 bp segment of the rpsL sequence from *Mycobacterium smegmatis*, and two different GC clamp lengths on the same end. (a) The rpsL sequence with a 25 bp GC clamp (163 bp DNA); (b) the same rpsL sequence with a 40 bp GC clamp (178 bp).

automate this process [12]. It calculates the melting map and derivative melting curve of overlapping DNA fragments that cover a sequence. The first base pair for each fragment length is incrementally advanced from one end of the sequence to the other in 10 bp steps. Fragment lengths are varied from 110 to 520 bp in 10 or 20 bp steps. The melting characteristics of each DNA fragment is analyzed to find the optimal fragment for detecting mutations in a designated segment of interest. The initial screening looks for fragments with two or more peaks in their DMC. Fragments with two or more peaks are stored and indexed by the base pairs in their first melting domain. The fragment which contains the region of interest in the first melting domain, a temperature separation between the first and second peaks in the DMC of at least 0.8°C, and the smallest first melting domain is the optimum fragment. The influence of adding GC clamps of varying lengths are theoretically evaluated if the natural sequence does not allow for mutation detection.

2.3. Use of end clamps to inhibit strand dissociation

2.3.1. GC clamps

The implications of the melting map pattern and the role of strands dissociations led Myers et al. [22] to introduce the idea of stabilizing one end of a DNA fragment by attaching a GC rich region, or GC clamp. Recombinant DNA techniques were employed to add a 300 bp GC rich sequence to a target fragment 135 bp long. The melting behavior of the fragment containing the target and clamp sequence placed the target sequence in a melting domain separated from strand dissociation. This procedure allowed the detection of 95 to 100% of possible base pair substitutions in the target fragment.

Sheffield et al. [6] used the polymerase chain reaction (PCR) to attach GC-clamps to DNA fragments. The addition of a string of G and C nucleotides to the 5′ end of one of the PCR primers provided a one step approach for stabilizing one end of a fragment. Amplification of genomic DNA by PCR also allowed visualization of gel bands with ethidium bromide staining. The length of the GC-clamp required to create melting behavior appropriate for detecting mutations can be assessed from the derivative melting curve. Fig. 5 shows the DMCs

of two DNAs containing the *Mycobacterium Smegmatis* rpsL sequence with either a 25 or 40 bp GC clamp. The 25 bp clamp produces a DMC indicating that the lowest melting domain unwinds just prior to the onset of strand dissociation. The 40 bp clamp increases the temperature difference between the two transition steps, and suggests a fragment more certain to detect mutations in the first melting domain.

Abrams et al. [7] developed a third method for attaching a GC clamp onto a genomic restriction fragment. The method uses a radioactively labeled single stranded probe which has the wild type copy of the genomic restriction fragment sequence and a GC clamp sequence on the 5′ end. An unlabeled restriction fragment from a genomic DNA sample is melted and annealed with the probe. DNA polymerization is used to fill in the GC clamp tail and create a completely duplex molecule. This approach enables one to directly examine genomic DNA fragments for mutations or modifications. Modifications such as base methylation can be detected.

2.3.2. Chemical clamps

An approach which completely removes the influence of duplex-strands dissociation on the melting behavior of a DNA is to crosslink the two strands. Costes et al. [34] and Fernandez et al. [35] introduced the use of a chemical crosslink clamp for TGGE and DGGE using psoralen and PCR. Psoralens are a class of naturally occurring heterocyclic compounds which can intercalate between bases in double stranded DNA. They are bifunctional photosensitive reagents that can form either a monoadduct or a diadduct with pyrimidine bases, predominantly thymidines. A crosslinked PCR product was made by modifying one of the primers. A psoralen derivative, 5-(ω-hexyloxy)psoralen, and a noncomplementary dApdA or dApdT sequence was attached to the primer's 5′ end. Upon exposure to UV light with wavelengths 320–400 nm, the psoralen derivative crosslinked the two strands by forming an adduct between the intercalated psoralen ring and a thymidine on the complementary strand. The crosslinking efficiency appears to vary from 50 to 85%. Aside from the potential complications due to interference of the noncrosslinked duplexes, the method provides a successful alternative to long GC-clamps. Wiese et al. [36] found strand dissociation completely suppressed in the psoralen clamped

strands. Bienvenu et al. [37] screened 21 sequences of the CFTR gene by gradient gel electrophoresis using psoralen clamps.

3. Recent applications of TGGE and related methods

3.1. Screening for mutations or polymorphisms

Denaturing gel electrophoresis methods have been applied in an increasing number of studies aimed at detecting mutations or polymorphisms. A recent search of a journal database found over 250 citations to denaturing gel electrophoretic methods during the past five years. The methods have been employed to screen for mutations in a variety of genes and with different purposes. A number of studies have screened for the presence of mutations in genes associated with human tumor formation. Genes examined include p53 [38–41], thyroid-stimulating hormone (TSH) receptor [42], T-cell receptor gamma chain [43], hMSH2 [44], IgH [45], and N-ras [46]. Analysis of viral genes of HIV-1 [47] and cytomegalovirus [48] has demonstrated the ability of TGGE to characterize viral sequence diversity in an infected individual. Denaturing gel methods have also been used to characterize mammalian [49,50] and bacterial populations [51].

The approach typically employed in the above studies is to select a 30–300 bp region where mutations or polymorphisms are anticipated, and then amplify a DNA fragment which has the region of interest in a low melting domain. Melting calculations are generally used to ascertain if a potential fragment has the region of interest in a low melting domain. We describe below studies on several different genes that illustrate the application of melting calculations and TGGE for detecting mutations and polymorphisms.

3.1.1. p53 gene mutations

The p53 gene is located at chromosome 17 in humans and encodes a 53 kd nuclear phosphoprotein involved in the control of cell growth. It is a tumor suppressor gene, and mutations in the p53 gene are among the most common genetic abnormalities reported in human cancers [52]. The vast majority of mutations found in the p53 gene from tumor cells are located in four highly conserved regions located in exons 5 through 8. We refer to these regions as mutational hot spots. Borresen et al. [38] first demonstrated the application of a variant of DGGE called constant denaturant gel electrophoresis (CDGE) in a study of p53 mutations in genomic DNA from tumor cells. CDGE employs a perpendicular DGGE to first determine the percentage of denaturant which partially melts the domain of interest. Constant denaturant gels are then run using this denaturant concentration.

Our laboratory carried out a study to screen for p53 mutations in PCR amplified fragments from cDNA as well as genomic DNA [23,53]. The genomic DNA and mRNA samples were isolated from human leukemic T-cell lines, and from bone marrow cells obtained from two patients with acute lymphoblastic leukemia [53]. Previous work indicated that 60% or more of human leukemic T-cell lines have mutations in the p53 gene, and that p53 mutations are associated with the relapse phase of acute lymphoblastic leukemia [54]. This work provided a test of the MELTSCAN program and TGGE method.

The first step was to predict which DNA fragments would allow detection of mutations in the four hot spot regions of the p53 gene. The four hot spot regions are designated A, B, C and D, and encompass codons 128–153 (A), 161–185 (B), 236–253 (C), and 265–301 (D) [52]. Fragments were initially selected for the cDNA sequence based on iterative calculation and inspection of melting maps and derivative melting curves using the criteria described above [23]. Analysis using the MELTSCAN program produced essentially identical results [12]. Mutations in the four hot spots of the cDNA sequence were predicted to be detectable using three fragments; 310 bp A-fragment (positions 311–600 with a 20 GC clamp below 311), 140 bp B-fragment (positions 581–690 with a 20 GC clamp below 581), and 410 bp C/D-fragment (positions 611–1000 with a 20 GC clamp below 611). Positions refer to the base pair number of the cDNA sequence [55].

MELTSCAN was also employed to select fragments from the genomic DNA sequence of the p53 gene [12]. Fragments were predicted for three of the four hot spots using 20 or 25 bp GC clamps. The

fragment for hot spot A required a 40 bp GC clamp. The four predicted DNAs were a 120 bp gA-fragment (positions 13 061–13 140 with 40 bp GC clamp below 13 061), 140 bp gB-fragment (positions 13 131–13 245 with 25 bp GC clamp below 13 131), 210 bp gC-fragment (positions 13 926–14 110 with 25 bp GC clamp below 13 926) and 520 bp gD-fragment (positions 14 021–14 520 with 20 bp GC clamp below 14 021). Fig. 6 shows the melting map and derivative melting curve for the 210 bp gC-fragment.

The three predicted cDNA fragments were tested with eight single site mutations distributed among the four hot spots. PCR was used to amplify fragments from plasmids containing cDNA inserts with
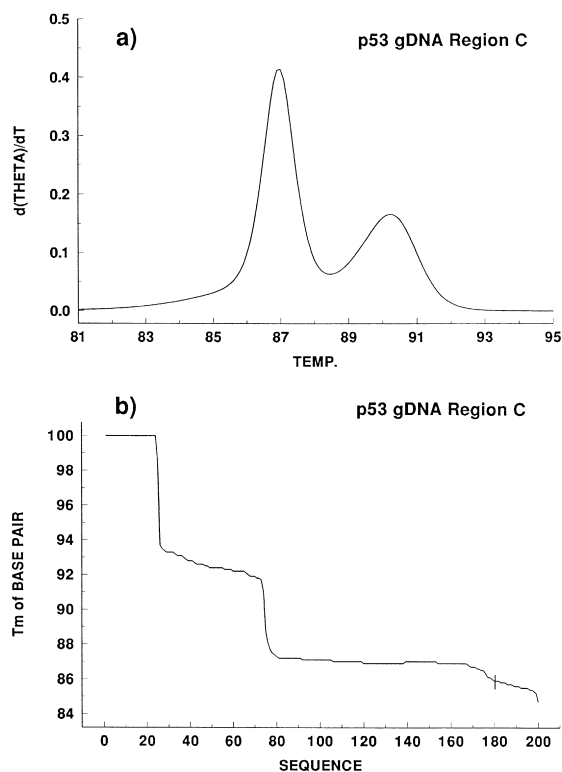

Fig. 6. The melting map and derivative melting curve of the 210 bp gC DNA fragment selected by MELTSCAN for hot spot C of the p53 gene. The fragment includes base positions 13 926 to 14 110 of the p53 gene and has a 25-bp GC clamp below 13 926. Hot spot region C covers base pair positions 133 to 188 in the figure (14 058 to 14 113 of the p53 gene). The location of the mutation detected in several samples is indicated by the vertical tick mark in the melting map curve.

the known mutations. The end points of the primer pairs predicted by MELTSCAN were moved up to 8 bases without compromising the fragments usefulness for detecting mutations. This can be helpful in optimizing the primers for PCR. The midpoint temperature of a TGGE experiment in a 6.5% PAG with 58% denaturant was estimated by subtracting 46°C from the T_m of the predicted first peak in the derivative melting curve. This empirical relation was based on studies of several fragments [53]. Gradients of 4 to 8°C were employed. In all cases the mutant fragment separated from the corresponding wild type fragment in a manner expected from the predicted melting behavior [23].

TGGE was then employed to screen for p53 mutations in PCR amplified DNA fragments derived from 13 T-cell lines, and cells from two patients. The DNA fragments were generated either from total mRNA extracts by reverse transcription and polymerase chain reaction, RT/PCR, or from PCR amplifications of extracted genomic DNA. All T-cell lines were screened for point mutations in all four hot spots using the three cDNA fragments. Genomic DNA samples were screened for mutations in hot spots B and C using the predicted gDNA fragments in seven of the cell lines. The results on the cDNA fragments from the T-cell lines are summarized in Table 1. Seven of the thirteen cell lines showed a mutation in either the B or C/D regions, and two cell lines showed mutations in both the B and C/D fragments. Both patient samples showed mutations in hot spot region B. Results from the genomic DNA fragments were consistent with the results from the cDNA fragments.[1]

Fig. 7 shows a typical TGGE experiment from this study. Six samples were examined using the PCR amplified 140 bp B-fragment. Heterozygosity is displayed in lanes 3 through 6 where four bands are observed. The two slower moving bands are due to the melted and annealed wild type and mutant fragments that produced DNAs with mismatched base pairs. The TGGE results verified previous work on three of the cell lines (Namalwa, HSB2 and CEM), and were confirmed by direct sequencing of

---

[1]Initial results on genomic DNA and cDNA p53 fragments indicated an inconsistency (ref. [53]) which was resolved by later experiments.

Table 1
Mutation detection of cDNA samples of the p53 gene

Sample	A, 280 bp 304 bp	B, 140 bp	C/D 440 bp	Sequence changes
REH	–	–	–	
207CL	–	Hetero	–	
858	–	–	–	
697	–	–	–	
6TCEM-20[d1]	–	Homo	–	
CEM[d2]	–	Hetero	Hetero	Codon 175 G→A, Codon 248 G→A[b]
HSB2[d3]	–	–	–	Not found[b]
Raji[d4]	–	–	Homo	
91-17CL	–	Hetero	Hetero	Codon 248 G→A[a]
920	–	–	Homo	Codon 273 G→T[a]
LT	–	–	–	
Namalwa[d5]	–	–	Homo	Codon 248 G→A, C→T[c]
B13	–	–	–	

The cDNA was generated by reverse transcription of mRNA isolated from cultured cell lines.

Hetero: heterogeneity, presence of two species of DNA, wt and mutant.

Homo: homozygosity, presence of single mutant species of DNA.

CL: sample from cultured cell line.

[a] Ref. [62].

[b] Ref. [63].

[c] Ref. [64].

[d] From ATCC: D1, CCL-119.1; d2, CCL-119; d3, CCL-120.1; d4, CCL-86; d5, CRL-1432.
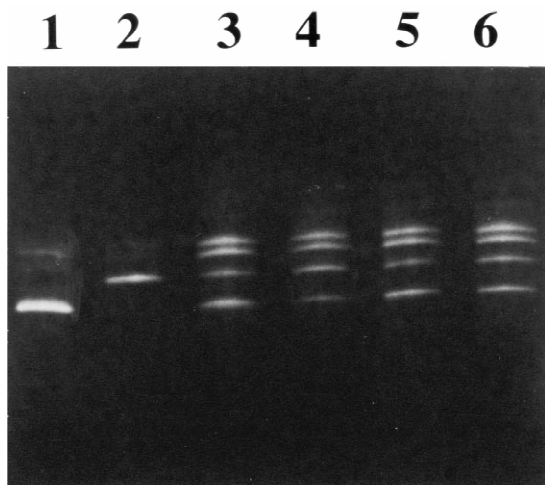

Fig. 7. Parallel TGGE experiment comparing 140 bp B-fragments amplified by PCR from several samples of p53 gene cDNAs. A temperature gradient of 43 to 53°C was used. The samples were run at 150 V for 5 h. Lanes and DNA samples; (1) wild type, (2) a characterized mutation in codon 175 (G659A[22]) of the p53 gene, (3) 207 cell line, (4) 91-17 cell line, (5) 91-17 patients bone marrow, (6) 207 patient's bone marrow.

DNA fragments from cell lines 91-17 and 920 (see Table 1). The frequency of the p53 mutations in the human leukemic T-cell lines was consistent with previous observations [54].

Except for the 120 bp gA fragment, the GC content of the p53 sequences described above were less than 52%, and required GC clamps 25 bp or shorter. The 120 bp gA fragment was predicted to require a longer GC clamp since the sequence of interest had a high GC content (61%), and was surrounded by GC rich sequences. Denaturing gradient gels may be adjusted to situations of high GC content by employing a longer GC clamp (or chemical clamp), and a higher percentage of denaturant in the gel. This situation was exemplified in an application that detected drug-resistant mutations in a bacterial gene with a high GC content.

3.1.2. Mutation detection in bacterial rpsL gene

The nonpathogenic mycobacterial organism *Mycobacterium smegmatis* is closely related to *Mycobacterium tuberculosis*, the bacteria responsible for tuberculosis. The rpsL gene of *M. smegmatis* encodes the ribosomal protein S12. Kenny and

Churchward [56] have shown the rpsL gene to be the primary site for spontaneous mutations that confer resistance to the antibiotic streptomycin. Twenty eight spontaneous mutations were characterized, and shown to partition among four different point mutations affecting codon 43, and four different point mutations affecting codons 86 or 88 or 91. The GC content of this gene is 64.9%. TGGE and MELTSCAN were employed to detect rpsL mutations known to confer streptomycin resistance.

MELTSCAN was utilized to select DNA fragment(s) which would allow for detection of mutations in the region around codon 43, and the region enclosing codons 86 to 91. Calculations predicted that two fragments would enable detection of mutations; a 163 bp DNA (positions 301–438 with a 25 GC clamp below 301) for the region surrounding codon 43, and a 320 bp DNA (positions 281 to 580 with a 20 bp GC clamp below 281). The melting map and derivative melting curve for the 163 bp DNA are described in Figs. 3 and 5a. The position of codon 43 is shown in the melting map. Although the derivative melting curve does not show a large separation between the first melting domain and the strands separation step, this fragment proved successful at detecting mutations.

Fragments were amplified by PCR from genomic *M. Smegmatis* DNA from wild type and streptomycin resistant strains. Due to the high GC content of the fragments, gels containing 68% denaturant were used. TGGE was able to separate the known mutations in codons 86 (CGT to CTT), 88 (AAG to AGG, and AAG to GAG) and 91 (CCC to CAC) from the wild type 320 bp fragment as well as from each other. A 44 to 54°C gradient was employed. Similarly, TGGE was able to separate the four different point mutations in codon 43 (AAG to AGG, AAC, AAT, or ACG) in the 163 bp DNA fragments using a 50 to 56°C gradient.

It is worth mentioning that the initial MELTSCAN calculation to find a fragment for detecting the 9 bp region surrounding codon 43 selected a fragment 360 bp long (positions 301 to 635 with a 25 GC clamp below 301). This fragment placed the codon 43 region at the border between the first two melting domains. Since preliminary TGGE experiments were not successful at separating a mutant from wild type fragment, the hot spot length surrounding codon 43

region was increased to 20 bp and the allowable fragment length was reduced. This decreased the separation between the two peaks in the derivative melting curve, but positioned the region of interest within a first melting domain away from a border. This is the only occasion out of 11 sequences examined so far in which MELTSCAN predicted a fragment that was unsuccessful at detecting a test mutation. It suggests that hot spots designated in MELTSCAN should be at least 20 bp long and that melting domain borders may not always be clearly predicted.

3.1.3. Screening for polymorphisms

Denaturing gel methods have also been employed to detect polymorphisms for gene mapping and population studies. The ability of TGGE and related methods to screen regions up to several hundred base pairs, and to distinguish the type of base pair change enhances its utility for populations studies. A method involving DGGE was developed to detect polymorphisms in human mitochondrial DNA [49]. Five fragments containing low melting domains 100–200 bp long were analyzed. The fragments covered segments in the genes for tRNA glycine/NADH dehydrogenase subunit III, cytochrome *c* oxidase subunit I, NADH dehydrogenase subunit III, and the replication origin site. Sequence variants were detected from PCR amplified fragments with mitochondrial DNA templates isolated from human T-cells. Campbell et al. [50] applied TGGE with heteroduplex analysis to detect polymorphisms in a 433 bp fragment of the mitochondrial DNA from Melomy cervinipes, a rodent.

We have employed TGGE to screen for a specific polymorphism in the Sry gene of mouse strains [57]. This gene encodes a regulatory protein that appears to be responsible for directing the pathway of sexual dimorphism in mammals [58]. MELTSCAN was applied to the 471 bp region surrounding the AT to GC polymorphism [59]. The GC content of the region is 47%. MELTSCAN predicted a 140 bp fragment should detect this polymorphism (positions 261 to 380 with a 20 bp GC clamp below 261). TGGE detected the polymorphic differences in PCR amplified DNA from the previously characterized mouse strains Poschiavinus and C57BL/6. The mobility difference

of the AT to GC substitution was detected in 6 out of 20 previously uncharacterized strains.

3.2. Temporal temperature gradient gel electrophoresis

A modification of the temperature gradient method was introduced by Yoshino et al. [60] in which the temperature of a gel plate was increasing gradually and uniformly with time. An advantage of this approach is that it requires only one thermostated fluid circulator. The circulator must have the capability to increase the temperature with time in a controlled manner. One must synchronize the electrophoretic mobility of the fragments to the rate of temperature increase. Penner and Betze [61], and Weise et al. [36] have developed variants of the temporal temperature gradient gel method in which the temperature decreases in a gradual and uniform manner.

The method employed by Weise et al. [36] combined a temporally decreasing temperature gradient gel together with psoralen clamped DNA fragments. Three DNA fragments were amplified from the human prion protein gene to detect mutations. They were chosen on the basis of melting map calculations, and predictions of the relative mobility difference between a crosslinked DNA with a mismatch, and the crosslinked wild type DNA. PCR reactions amplified the desired fragments using pairs of primers with one primer of each pair containing a 5′ psoralen derivative. Each sample fragment was melted and annealed with a wild type fragment to form a mixture of homoduplex DNAs, and heteroduplex molecules with mismatches. These four species were then crosslinked at one end through a psoralen adduct. DNA samples were loaded at a temperature sufficient to melt the DNAs, and electrophoresed for a period of time sufficient to separate the crosslinked from noncrosslinked DNAs. The heating device was then switched off, and the temperature of the buffer and fluid in the circulator were allowed to cool. The homoduplex and heteroduplex crosslinked DNAs separated from each other in accordance with their thermal stability. Ten previously characterized mutations in the human prion gene were detected using the three DNA fragments. Although the buffer volume in this system is large (4.5 liters), the use of psoralen clamped DNAs and the single fluid circulator provide advantages for mutation detection.

3.3. The influence of single site defects on DNA stability

In addition to its applications for mutation detection, TGGE can be used to evaluate the stability of DNA molecules carrying defects or base pair substitutions at single sites. The method compliments other approaches such as UV monitored solution denaturation and calorimetry of DNA oligomers. Small amounts of material are required for TGGE (1–5 µg), and long DNAs may be examined. The method has been employed to examine how nearest neighbor base pairs influence the stability of specific non-Watson–Crick base pairs and bulges. This information is of interest with regard to investigating the influence of mismatch stability on the formation of spontaneous mutations. It may also be relevant for methods such as TGGE and probe hybridization that rely on thermal stability differences to separate DNAs with similar sequences. Knowing how a mismatch or bulge and its neighboring base pairs effect DNA stability may help identify the nature of a mutation or polymorphism.

Ke and Wartell [8] examined the relative stability of all possible base pairs and mismatches at four positions within the first melting domain of the 373 bp DNA described in Fig. 3. Site directed mutagenesis by PCR was used to create DNAs with all four base pairs at a given site. Melting and annealing pairs of DNAs created the two homoduplexes and two heteroduplexes. Fig. 8 shows a parallel TGGE experiment of the 373 bp DNA with all paired and mismatched bases at the "X·Y" position 14 base pairs from the EcoRI end. The neighboring base pairs around this position are d(CXA)·d(TYG). The relative depths to which the different DNAs migrated in this gel delineate the relative stability of the base pairs and mismatches at this position. The temperature gradient employed, 29.0 to 32.5°C, enabled all bands to be observed. In order to further distinguish the mismatched DNAs, a temperature gradient centered at a lower temperature may be employed. The results of Fig. 8 illustrate the band patterns produced by melting and reannealing two DNA molecules
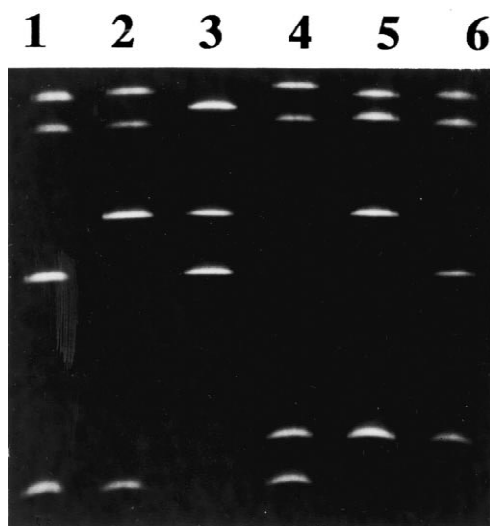
Fig. 8. Parallel TGGE experiment of the 373 bp DNA fragments differing by single base pair substitutions and mismatches at the position 14 bp away from the EcoRI end. The samples were run for 14 h at 80 V. A temperature gradient from 29.0 to 32.5°C was employed. From top to bottom in each lane, DNA bands correspond to the following pair of bases at position 14: (1) AC, GT, AT, GC; (2) TC, GA, TA, GC; (3) TT, AA, TA, AT; (4) CC, GG, CG, GC; (5) CA, TG, TA, CG; (6) CT, AG, AT, CG. (From Ref. [8], with permission).
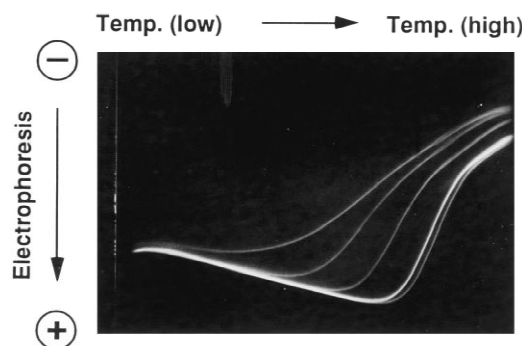

Fig. 9. Perpendicular TGGE experiment of several 373 bp DNA fragments. The samples were run for 14 h at 90 V. The temperature gradient was 17 to 35.5°C from left to right. The mobility curves from left to right correspond to DNAs with the following pair of bases at the position 14 bp in from the EcoRI end: CC, GG, TA, CG, GC. (From Ref. [8], with permission).

differing by a single base pair substitution. For example, lane 1 shows the pattern for a G·C to A·T mutation, while lane 4 shows a pattern for a G·C to C·G mutation. The different band patterns produced suggest a way to characterize or "fingerprint" a base pair change, thus providing useful information when screening for mutations or polymorphisms.

Fig. 9 shows a perpendicular TGGE experiment of several 373 bp DNAs differing by a base pair substitution or mismatch at the d(CXA)·d(TYG) site. The temperature gradient was chosen to display only the first melting domain of the DNAs. This type of experiment provides a means to quantify the stability differences between DNAs from the midpoints of the transitions, T_u. A mismatch decreased the stability of the first melting domain by 1 to 4°C. Results from the parallel and perpendicular TGGE experiments indicated that the influence of the 12 possible mismatches on DNA stability varies with the nearest neighbor environment, but depends predominantly on mismatch type. G·T, G·G and G·A pairs were always among the most stable mismatches, and

pyrimidine·pyrimidine mismatches were among the least stable.

Similar TGGE studies [9] were made to determine the effect of single base bulges, and base pair deletions on DNA stability. The 373 bp DNA containing a single base bulge was destabilized by an amount similar to the DNA with a mismatch. Purine bulges were generally not as destabilizing as pyrimidine bulges, however the neighboring base pair environment had a significant effect. An unpaired base identical to one of its adjacent bases caused less destabilization than an unpaired base with an identity differing from its neighbors. This is consistent with the idea that positional degeneracy of an unpaired base enhances the entropy of the DNA. Another outcome from this study was the observation that a deletion of a base pair always produced a DNA with a stability higher than the DNA with an A·T (or T·A) pair, and lower than the DNA with a G·C (or C·G) pair.

References

[1] D. Riesner, K. Henco, G. Steger, in: A. Chrambach, M. Dunn, B.J. Radola (Eds.), Advances in Electrophoresis, Vol. 4, VCH, New York, 1991, p. 171.

[2] L.S. Lerman, S.G. Fischer, I. Harley, K. Silverstein, N. Lumelsky, Annu. Rev. Biophys. Bioeng. 13 (1984) 399.

[3] L.S. Lerman, K. Silverstein, Methods Enzymol. 155 (1987) 482.

[4] R.M. Myers, T. Maniatis, L.S. Lerman, Methods Enzymol. 155 (1987) 501.

[5] E.S. Abrams, V.P. Stanton Jr., Methods Enzymol. 212 (1992) 71.

[6] V.C. Sheffield, D.R. Cox, L.S. Lerman, R.M. Myers, Proc. Nat. Acad. Sci. USA 86 (1989) 232.

[7] E.S. Abrams, L.S. Lerman, Genomics 7 (1990) 163.

[8] S.-H. Ke, R.M. Wartell, Nucleic Acids Res. 21 (1993) 5137.

[9] S.-H. Ke, R.M. Wartell, Biochemistry 34 (1995) 4593.

[10] R.M. Wartell, A.S. Benight, Phys. Rep. 126 (1985) 67.

[11] O. Gotoh, Y. Tagashira, Biopolymers 20 (1981) 1033.

[12] S. Brossette, R.M. Wartell, Nucleic Acids Res. 22 (1994) 4321.

[13] G. Steger, Nucleic Acids Res. 22 (1994) 2760.

[14] C.J. Weber, D.J. Shaffer, C.L. Sidman, Nucleic Acids Res. 12 (1991) 333.

[15] E. Hovig, B. Smith-Sorensen, A. Brogger, A. Borresen, Mutation Res. 262 (1991) 63.

[16] C. Schlotterer, Electrophoresis 16 (1995) 722.

[17] D. Thatcher, B. Hodson, Biochem. J. 197 (1981) 105.

[18] V. Rosenbaum, D. Riesner, Biophys. Chem. 26 (1987) 235.

[19] R.M. Wartell, S.H. Hosseini, J.D. Moran, Nucleic Acids Res. 18 (1990) 2699.

[20] D.M. Crothers, T.E. Haran, J.G. Nadeau, J. Biol. Chem. 13 (1990) 7093.

[21] E.S. Abrams, S.E. Murdaugh, L.S. Lerman, Nucleic Acids Res. 14 (1995) 2775.

[22] R.M. Myers, S.G. Fischer, L.S. Lerman, T. Maniatis, Nucleic Acids Res. 13 (1985) 3131.

[23] S.-H. Ke, P.J. Kelly, R.M. Wartell, S.H. Hunter, V.A. Varma, Electrophoresis 14 (1993) 561.

[24] R.M. Myers, S.G. Fischer, T. Maniatis, L.S. Lerman, Nucleic Acids Res. 13 (1985) 3111.

[25] S.G. Delcourt, R.D. Blake, J. Biol. Chem. 266 (1991) 15160.

[26] W. Hillen, T.C. Goodman, A.S. Benight, R.M. Wartell, R.D. Wells, J. Biol. Chem. 6 (1980) 2761.

[27] A. Suyama, A. Wada, Biopolymers 23 (1981) 409.

[28] S.A. Kozyavkin, Y.L. Lyubchenko, Nucleic Acids Res. 10 (1984) 4339.

[29] S.C. Hardies, W. Hillen, T.C. Goodman, R.D. Wells, J. Biol. Chem. 20 (1979) 10128.

[30] R.D. Blake, S.G. Delcourt, Nucleic Acids Res. 11 (1996) 2095.

[31] H. Klump, W. Burkart, Biochim. Biophys. Acta 475 (1997) 601.

[32] F. Michel, J. Mol. Biol. 89 (1974) 305.

[33] M.P. Perelroyzen, V.I. Lyamichev, Yu.A. Kalambet, Yu.L. Lyubchenko, A.V. Vologodskii, Nucleic Acids Res. 9 (1981) 4043.

[34] B. Costes, E. Girodon, N. Ghanem, M. Chassignol, N.T. Thuong, D. Dupret, M. Goossens, Hum. Mol. Genet. 2 (1993) 393.

[35] E. Fernandez, T. Bienvenu, F. Desclaux, K. Arramond, J. Beldjord, C. Kaplan, C. Beldjord, PCR Methods Appl. 3 (1993) 122.

[36] U. Wiese, M. Wulfert, S.B. Prusiner, D. Riesner, Electrophoresis 16 (1995) 1851.

[37] T. Bienvenu, C. Cazeneuve, J.C. Kaplan, C. Beldjord, Hum. Mutat. 6 (1995) 23.

[38] A.-L. Borresen, E. Hovig, B. Smith-Sorensen, D. Malkin, S. Lystad, T.I. Andersen, J.M. Nesland, K.J. Isselbacher, S.H. Friend, Proc. Nat. Acad. Sci. USA 88 (1991) 8405.

[39] R. Seruca, L. David, S. Castedo, I. Veiga, A.L. Borresen, M. Sobrinho-Simoes, Cancer Genet. Cytogenet. 75 (1994) 45.

[40] K. Kusama, S. Okutsu, A. Takeda, T. Himiya, A. Kojima, Y. Kidokoro, L. Chu, S. Iwanari, I. Kudo, I. Moro, J. Pathol. 178 (1996) 415.

[41] M. Pocard, S. Chevillard, J. Villaudy, M.F. Poupon, B. Dutrillaux, Y. Remvikos, Oncogene 12 (1996) 875.

[42] M. Koch, R. Whal, F.J. Seif, Electrophoresis 16 (1995) 742.

[43] I. Theodorou, C. Bigorgne, M.H. Delfau, C. Lahet, G. Cochet, M. Vidaud, M. Raphel, P. Gaulard, J.P. Farcet, J. Pathol. 3 (1996) 303.

[44] A.-L. Borresen, R.A. Lothe, G.I. Meling, S. Lystad, P. Morrision, J. Lipford, M.F. Kane, T.O. Rognum, R.D. Kolodner, Hum. Mol. Genet. 4 (1995) 2065.

[45] B. Linke, J. Pyttlich, M. Tiemann, M. Suttorp, R. Parwaresch, W. Hiddemann, M. Kneba, Leukemia 9 (1995) 840.

[46] M. Ridanpaa, K. Burvall, L.H. Zhang, K. Husgafel-Puriainen, A. Onfelt, Mutat. Res. 334 (1995) 357.

[47] U. Wieland, B. Suhr, B. Salzberger, H.J. Eggers, R.W. Braun, J.E. Kuhn, J. Virol. Methods 2 (1996) 127.

[48] J.E. Kuhn, T. Wendland, H.J. Eggers, E. Lorentzen, B. Wieland, B. Eing, M. Kiessling, P. Gass, J. Med. Virol. 47 (1995) 70.

[49] J.S. Hanekamp, W.G. Thilly, M.A. Chaudhry, Hum. Genet. 98 (1996) 243.

[50] N.J. Campbell, F.C. Harriss, M.S. Elphinstone, P.R. Baverstock, Mol. Ecol. 4 (1995) 407.

[51] M.J. Ferris, G. Muyzer, D.M. Ward, Appl. Environ. Microbiol. 62 (1996) 340.

[52] M. Hollstein, D. Sidransky, B. Vogelstein, C.C. Harris, Science 253 (1991) 49.

[53] S. Hosseni, Ph.D. Dissertation, Georgia Institute of Technology, Atlanta, GA, 1994.

[54] J. Yeargin, J. Cheng, A.L. Yu, R. Gjerset, M. Bogart, M. Haas, J. Clin. Inv. 91 (1993) 2111.

[55] R. Zakut-Houri, B. Bienz-Tadmor, D. Givol, M. Oren, EMBO J. 4 (1985) 1251.

[56] T.J. Kenney, G.J. Churchward, J. Bacteriol. 176 (1994) 6153.

[57] S.C. Powell, V. Gupta, J.B. Whitney, R.M. Wartell, unpublished results.

[58] C.M. Haqq, C. King, S.F. Ukiyama, T.N. Haqq, P.K. Donahoe, M.A. Weiss, Science 266 (1994) 1494.

[59] J. Gubbay, J. Collignon, P. Koopman, A. Economou, A. Munsterberg, N. Vivian, P. Goodfellow, R. Lovell-Badge, Nature 346 (1990) 245.

[60] K. Yoshino, K. Nishigaki, Y. Husimi, Nucleic Acids Res. 11 (1991) 3153.

[61] G. Penner, L. Bezte, Nucleic Acids Res. 9 (1994) 1780.

[62] C. Zhou, H. Findley, Emory University, personal communication.

[63] J. Cheng, M. Haas, Mol. Cell Biol. 10 (1990) 5502.

[64] G. Giadano, P. Ballerini, J.Z. Gong, G. Inghirami, A. Neri, E. Newcombs, I.T. Magrath, D.M. Knowles, R. Dalla-Favera, Proc. Nat. Acad. Sci. USA 88 (1991) 5413.